Interface fluctuations for deposition on enlarging flat substrates

New Journal of Physics
The open access journal at the forefront of physics
Deutsche Physikalische Gesellschaft DPG | IOP Institute of Physics

Interface fluctuations for deposition on enlarging flat substrates

I S S Carrasco[1], K A Takeuchi[2], S C Ferreira[1] and T J Oliveira[1,3]

[1] Departamento de Física, Universidade Federal de Viçosa, 36570-000, Viçosa, Minas Gerais, Brazil
[2] Department of Physics, The University of Tokyo, 7-3-1 Hongo, Bunkyo-ku, Tokyo 113-0033, Japan
E-mail: tiago@ufv.br

Received 16 September 2014, revised 6 November 2014
Accepted for publication 18 November 2014
Published 22 December 2014

New Journal of Physics **16** (2014) 123057

doi:10.1088/1367-2630/16/12/123057

Abstract

We investigate solid-on-solid models that belong to the Kardar–Parisi–Zhang (KPZ) universality class on substrates that expand laterally at a constant rate by duplication of columns. Despite the null global curvature, we show that all investigated models have asymptotic height distributions and spatial covariances in agreement with those expected for the KPZ subclass for curved surfaces. In 1 + 1 dimensions, the height distribution and covariance are given by the GUE Tracy–Widom distribution and the Airy_2 process instead of the GOE and Airy_1 foreseen for flat interfaces. These results imply that when the KPZ class splits into curved and flat subclasses, as conventionally considered, the expanding substrate may play a role equivalent to, or perhaps more important than, the global curvature. Moreover, the translational invariance of the interfaces evolving on growing domains allowed us to accurately determine, in 2 + 1 dimensions, the analog of the GUE Tracy–Widom distribution for height distribution and that of the Airy_2 process for spatial covariance. Temporal covariance is also calculated and shown to be universal in each dimension and in each of the two subclasses. A logarithmic correction associated with the duplication of columns is observed and theoretically elucidated. Finally, crossover between regimes with fixed-size and enlarging substrates is also investigated.

[3] Author to whom any correspondence should be addressed.

Keywords: surface growth, interface fluctuations, Kardar–Parisi–Zhang class

1. Introduction

The kinetic roughening of interfaces has attracted a lot of attention in recent decades [1, 2]. Most of the works are devoted to interfaces with a flat asymptotic shape due to their close relationship to technological applications such as, for example, thin film growth [3, 4]. However, kinetic roughening with curved asymptotic shapes appears in a number of important physical systems, including biological growth [5], topological-defect turbulence of nematic liquid crystals [6, 7] and colloidal deposition at edges of evaporating drops [8].

It is well accepted that the scaling exponents of curved and flat interfaces are the same within each universality class [6, 7, 9–12], but the underlying fluctuations, in general, may depend on geometry and/or boundary conditions [6, 7, 13–15]. Prahöfer and Spohn [13] obtained an exact solution to the polynuclear growth (PNG) model in $d = 1 + 1$ dimensions, in which a single seed at the origin as the initial condition produces a macroscopically curved interface with fluctuations given by the Tracy–Widom (TW) distribution [16] for the Gaussian unitary ensemble (GUE). Otherwise, using a line as the initial condition, the resulting interface is macroscopically flat and the TW distribution for the Gaussian orthogonal ensemble (GOE) is found for underlying interface fluctuations.

The PNG model is known to be in the Kardar–Parisi–Zhang (KPZ) universality class, represented by the celebrated KPZ equation [17]:

$$\frac{\partial h}{\partial t} = \nu \nabla^2 h + \frac{\lambda}{2}(\nabla h)^2 + \xi, \tag{1}$$

where $h(x, t)$ is the height variable and ν, λ, and $\xi(x, t)$ account, respectively, for the surface tension, the amplitude of nonlinear effects, and a white noise with $\langle \xi(x, t) \rangle = 0$ and $\langle \xi(x, t)\xi(x', t') \rangle = 2D\delta(x - x')\delta(t - t')$. The different height distributions for curved and flat interfaces in the PNG model imply that the KPZ class splits into at least two subclasses, separating the curved and flat growth [13]. Indeed, this conjecture has been confirmed recently in experiments on the topological-defect turbulence of liquid crystals [6, 7] and in numerical simulations of models in the KPZ class [15, 18–20]. The same conclusion has also been reached analytically for a few other solvable models [14][3] and in particular for the one-dimensional KPZ equation [21].

The compilation of all results leads to the following expression, hereafter called the KPZ ansatz:

$$h \simeq v_\infty t + s_\lambda (\Gamma t)^\beta \chi + \eta + \ldots, \tag{2}$$

[3] Rounded facet edges of three-dimensional crystals are also known to exhibit the GUE TW distribution and other properties directly linked to the one-dimensional KPZ class [53–55]. However, we note that this corresponds to a situation rather different from ours because the facet edges are driven by thermal fluctuations under the constraint of volume conservation and confinement between atomic layers, and these are essential for the above properties to arise [53]. In contrast, here we study interfaces driven by athermal growth processes, such as atomic deposition, without such conservation and confinement. Therefore, it is not clear if one can draw any implications for facet fluctuations from the results presented in this paper, which is certainly an interesting question to ask.

where v_∞ and Γ are model-dependent constant parameters, s_λ is the sign of λ in the KPZ equation (1), and χ and η are stochastic variables. The scaling exponent β and the normalized fluctuations χ are expected to be universal. In particular, for $1 + 1$ dimensions, analytical, numerical, and experimental studies have shown that $\chi = \chi_2 \equiv \chi_{\rm GUE}$ for curved interfaces and $\chi = \chi_1 \equiv 2^{-2/3}\chi_{\rm GOE}$ for flat ones, where $\chi_{\rm GUE}$ and $\chi_{\rm GOE}$ are the standard random variables to describe the corresponding TW distributions [6, 7, 13–15]. The applicability of the ansatz (2) to $2 + 1$ dimensions, with distinct universal distributions for flat and curved growth, was recently reported [22–24] and experimentally verified, for the flat case, in the growth of semiconductor [25] and organic [26] films. Furthermore, equation (2) was numerically shown to hold for the restricted solid-on-solid (RSOS) model in dimensions d at least up to $d = 6 + 1$ [27].

Evolving curved interfaces investigated up to now are hallmarked by both macroscopic curvatures and expanding activity domains, whereas in flat growth this domain size (the substrate size) is kept constant. Therefore, a basic question arises: Is the curvature responsible for the appearance of the different distributions in the KPZ class, or is it the expanding growth domain that drives the height fluctuations to the different universal distributions? To address this question, we study standard flat-interface models in the KPZ class on substrates whose lateral size increases at a constant rate ω but the macroscopic curvature is kept null. Scaling exponents for interface growth models on expanding domains were recently analyzed [10, 28, 29]. Since the spatial correlation length increases as $\xi_\parallel \sim t^{1/z}$, where z is the dynamic exponent, for a substrate increasing as $L \sim t^\gamma$, the interface width evolves indefinitely as $W \sim t^\beta$ if $\gamma = 1 > 1/z$, because correlation length never reaches the system size [28]. Otherwise, for $\gamma < 1/z$ the surface becomes completely correlated ($\xi \sim L$) after a crossover time and the interface width scales as $W \sim t^{\gamma\alpha}$ [28], where $\alpha = \beta z$ is the roughness exponent. Similar behavior was found in an analytical study of linear growth equations on growing domains [29]. Masoudi *et al* [10] analyzed some typical flat models on substrates which grow at a constant rate ($\gamma = 1$), by alternating deposition and substrate enlargement deterministically, and they obtained the same growth exponents as for the fixed-size case.

In this work, the substrate enlargement is performed stochastically by duplicating randomly selected columns at a rate ω in addition to the usual deposition rules. We show that expanding systems exhibit height distributions given by the GUE TW distribution in $d = 1 + 1$ and its counterpart in $d = 2 + 1$, showing that they belong to the same KPZ subclass as the curved interfaces. This is also confirmed by the spatial covariance, given by the Airy_1 and Airy_2 processes for the fixed and growing domains, respectively, in $d = 1 + 1$, and their counterparts in $d = 2 + 1$. Universality in temporal covariance is also shown in $d = 1 + 1$ and $2 + 1$, again, with different universal functions for the different KPZ subclasses. The duplication mechanism introduces logarithmic corrections into the KPZ ansatz, which are explained with an approximate theoretical analysis. Furthermore, analyzing the effects of the initial size of the substrate, we characterize crossover from the fixed-size (GOE in $1 + 1$) to the enlarging substrate (GUE in $1 + 1$) regimes.

This paper is organized as follows. In section 2 we define the studied models and the method of substrate expansion. Sections 3 and 4 present the height distribution analysis for one- and two-dimensional substrates, respectively. The spatial and temporal covariances are presented in sections 5 and 6, respectively, and the crossover effect controlled by the initial substrate size is presented in section 7. Section 8 summarizes our conclusions and final discussions.

2. Growth models on enlarging domains

We study the restricted solid-on-solid (RSOS) [30], single-step (SS) [1], and etching [31] models on enlarging substrates represented by chains in $d = 1 + 1$ and square lattices in $d = 2 + 1$, with periodic boundary conditions. In all models, particles are added at a randomly chosen site i according to the following rules: RSOS—if $h_j - h_i = 0$ or 1 for $\forall\, j \in \mathcal{N}(i)$, then $h_i \to h_i + 1$ (so that $|h_j - h_i| \leqslant 1$ is always satisfied); SS—if $h_j - h_i = 1$ for $\forall\, j \in \mathcal{N}(i)$, then $h_i \to h_i + 2$; etching—$h_i \to h_i + 1$ and, if $h_j < h_i - 1$, then $h_j \to h_i - 1$ for each $j \in \mathcal{N}(i)$. Here $\mathcal{N}(i)$ represents the set of the nearest neighbors (NN) of i. Flat initial conditions, $h_i = 0$, were used for the RSOS and etching models, whereas chessboard initial conditions, h_i alternating between 0 and 1, were used for the SS model. Note that the SS model is identical to the BCSOS model studied by van Beijeren [32], where only the nearest neighbor interactions of the BCSOS model are taken into account.

The substrate enlargement is implemented as follows. A particle deposition is attempted with probability $P_d = N/(N + \omega d_s)$ whereas a column duplication occurs with complementary probability $P_a = \omega d_s/(N + \omega d_s)$, where N is the number of the lattice sites and d_s is the substrate dimension. After each event, time is increased by $\Delta t = 1/(N + \omega d_s)$. The initial lateral substrate size is L_0. In $d = 1 + 1$, each substrate enlargement is implemented by a simple local duplication of a randomly selected column for the RSOS and etching models, as illustrated in figure 1(a). In $d = 2 + 1$, a lattice row or column is randomly selected and similarly duplicated, as illustrated in figure 1(c). The lateral lattice size increases on average, therefore, as $\langle L \rangle = L_0 + \omega t$. In the SS model, we must duplicate a pair of NN columns at the same time to conserve the steps at the surface; see figure 1(b). Therefore, the substrate enlarging rate is 2ω.

Let us illustrate a consequence of the column duplication for the KPZ ansatz by an approximate argument. Let ∇h_i be the local gradient on a d_s-dimensional substrate so that $(\nabla h_i)^2 = \left(\frac{\partial h_i}{\partial x_1}\right)^2 + \left(\frac{\partial h_i}{\partial x_2}\right)^2 + \cdots + \left(\frac{\partial h_i}{\partial x_{d_s}}\right)^2$, where x_j with $j = 1, \cdots, d_s$ are the substrate directions. The mean squared gradient at time t is

$$G_t = \frac{1}{L^{d_s}} \sum_{i=1}^{L^{d_s}} (\nabla h_i)^2.$$

After ω duplications, in a time unity, we have

$$G_{t+1} = \frac{1}{(L+\omega)^{d_s}} \left[\sum_{i=1}^{L^{d_s}} (\nabla h_i)^2 + \sum_{i=1}^{(L+\omega)^{d_s} - L^{d_s}} (\nabla h_i)^2 \right], \tag{3}$$

where the first and second sums are taken over non-duplicated and duplicated sites, respectively. Considering only the effects of duplication and using the statistical equivalence of sites, we have

$$\sum_{i=1}^{L^{d_s}} (\nabla h_i)^2 \simeq L^{d_s} G_t$$

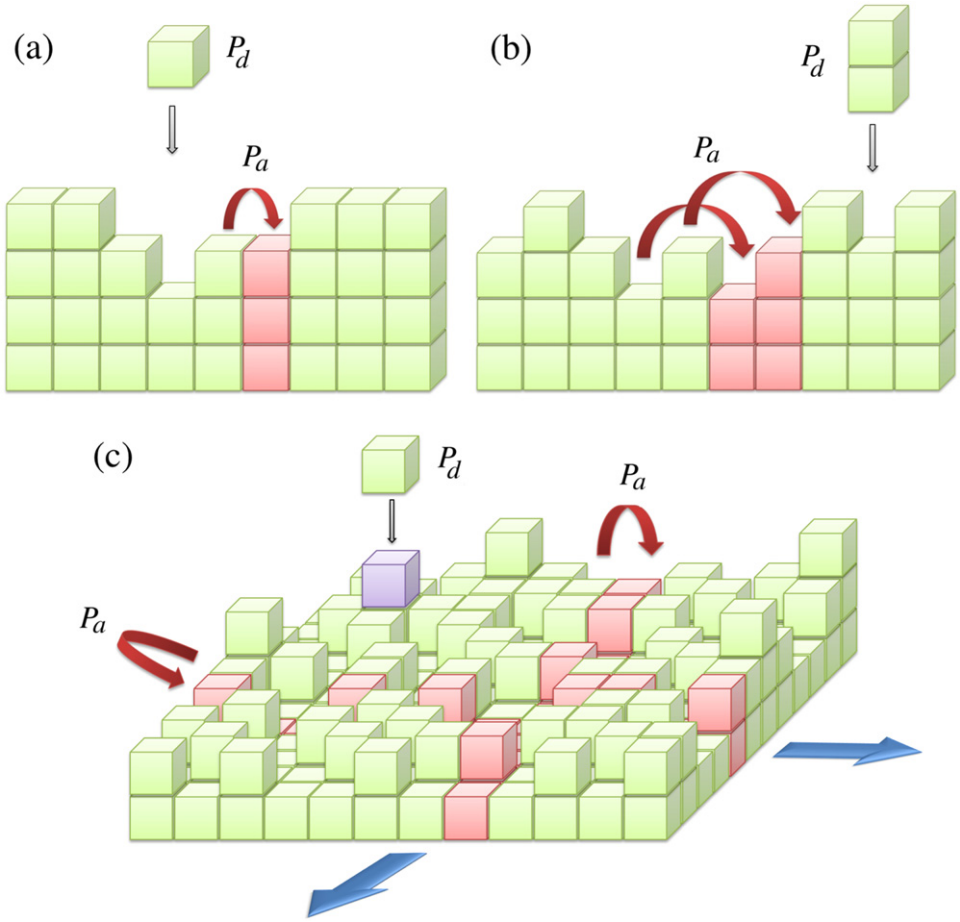

Figure 1. Illustration of the substrate enlargement and deposition for (a) the RSOS and (b) the SS model in 1 + 1 and in (c) 2 + 1 dimensions.

and

$$\sum_{i=1}^{(L+\omega)^{d_s}-L^{d_s}} \left(\nabla h_i\right)^2 \approx \frac{(d_s-1)}{d_s}\left[(L+\omega)^{d_s}-L^{d_s}\right]G_t,$$

where the ratio $(d_s - 1)/d_s$ appears because column duplication in the direction x_k implies $\left(\frac{\partial h_i}{\partial x_k}\right)^2 = 0$ along this column immediately after duplication. Inserting this result in equation (3) and considering long times so that $L \sim \omega t$, we find

$$G_{t+1} \approx \left\{1 + \frac{1}{d_s}\left[-1 + \frac{1}{(1+1/t)^{d_s}}\right]\right\}G_t.$$

Therefore, disregarding the terms $\mathcal{O}(t^{-2})$ for $t \gg 1$, we have

$$G_{t+1} - G_t \approx -\frac{1}{t}G_t \qquad \text{or} \qquad \frac{\mathrm{d}G}{\mathrm{d}t} \approx -\frac{1}{t}G,$$

implying $G_t \sim 1/t$ due to substrate expansion. It is unclear whether the column duplication produces the same effect when particle deposition is also considered, but the simplest scenario

would be to assume that the preceding functional form of G_t describes an additive correction to the height evolution (1), induced by the column duplication. This implies the presence of a logarithmic correction to the KPZ ansatz (equation 2), which now reads

$$h \simeq v_\infty t + s_\lambda(\Gamma t)^\beta \chi + \eta + s_\lambda \zeta \ln t + \ldots \tag{4}$$

where ζ is, in principle, a stochastic variable. We will see that this logarithmic correction indeed exists in all models and dimensions we investigated, and that the fluctuations of ζ, if they exist, are very small.

Note, however, that this logarithmic correction is predicted for KPZ-class interfaces on expanding substrates and not necessarily for other universality classes. More important, one can easily see that the duplication of a column does not induce any curvature in the global scale, i.e.,

$$\langle \nabla^2 h \rangle = 0,$$

which is guaranteed here by the choice of the periodic boundary condition. This allows us to study the effect of substrate expansion on KPZ universal fluctuations, independently of the global curvature.

3. Height fluctuations in 1+1 dimensions

This section presents numerical results for one-dimensional enlarging substrates, with $L_0 = \omega$ and up to 25 000 realizations. Figure 2(a) shows the effective growth exponent, defined by $\beta_{\rm eff}(t) \equiv \frac{1}{2}\frac{{\rm d}(\log \langle h^2 \rangle_c)}{{\rm d}(\log t)}$ with the second-order cumulant $\langle h^2 \rangle_c$, for all investigated models and two different values of ω. Convergence to the expected KPZ value $\beta = 1/3$ is found in all cases, in agreement with previous simulations of KPZ models in linearly growing domains, $L \sim t$ [10, 28].

To characterize the asymptotic height distributions, we analyzed the dimensionless cumulant ratios $S = \langle h^3 \rangle_c / \langle h^2 \rangle_c^{3/2}$ (skewness) and $K = \langle h^4 \rangle_c / \langle h^2 \rangle_c^2$ (kurtosis), where $\langle h^n \rangle_c$ is the nth-order cumulant of h. The results are plotted in figure 2(b) as functions of $t^{-2\beta}$, which is an expected functional form for their finite-time correction, usually obtained on the basis of the correction of $\mathcal{O}(t^{-2\beta})$ in the second-order cumulant [7, 15, 20, 33]. Our results indeed underpin this finite-time correction, and, extrapolating the data, we find that the asymptotic skewness and kurtosis indicate the values for the GUE TW distribution. We conclude, therefore, that the underlying distribution behind the asymptotic height fluctuations is given by the GUE TW distribution rather than the GOE counterpart found for $\omega = 0$. It is important to emphasize that the global curvature of the interface is not changed by duplications and remains identically null due to the periodic boundary conditions.

As $t \to \infty$, the number of the sites duplicated during each time unit becomes negligible compared with that of the non-duplicated sites. Therefore, the non-universal parameters such as v_∞, λ, and Γ should not be changed by substrate expansion. This implies that it is sufficient for us to determine them for the non-expanding case, $\omega = 0$. For the RSOS model, $v_\infty = 0.419030(3)$ and $\Gamma = 0.252(1)$ were numerically estimated in [15, 20]. The exact values of these quantities for the SS model are $v_\infty = \Gamma = 1/2$ [34]. Following the same procedures as in [19, 20], we found $v_\infty = 2.13986(5)$ and $\Gamma = 4.90(9)$ for the etching model. All these results were obtained for $\omega = 0$, but the validity of these values for the expanding case was explicitly verified.

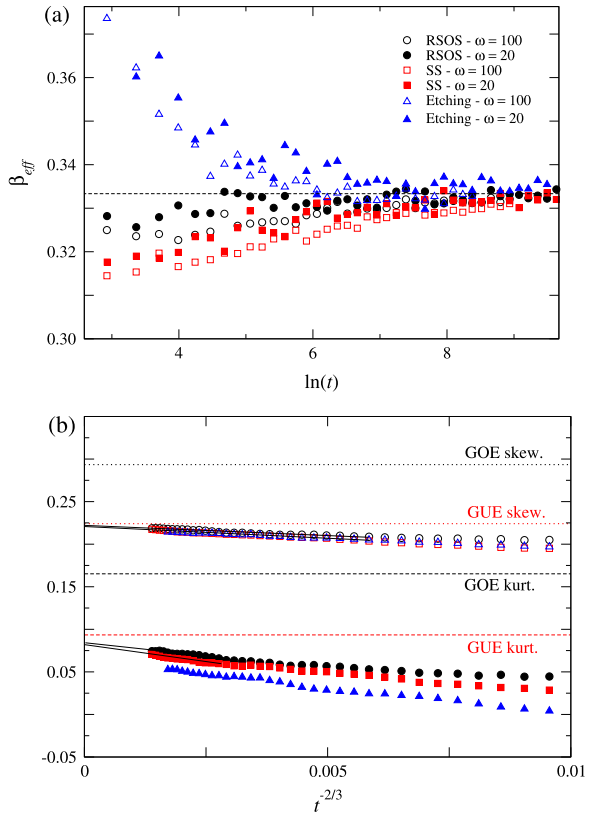

Figure 2. (a) Effective growth exponent as a function of $\ln(t)$. (b) Skewness (open symbols) and kurtosis (solid symbols) of the height distributions for the RSOS (black circles), SS (red squares), and etching (blue triangles) models, with $\omega = 20$. The dashed and dotted horizontal lines indicate the expected values of S and K for the GUE and GOE TW distributions, respectively.

According to equation (2), we have

$$\partial_t \langle h \rangle \simeq v_\infty + s_\lambda \beta \Gamma^\beta \langle \chi \rangle t^{\beta-1}.$$

Consequently, plotting $\partial_t \langle h \rangle$ against $t^{\beta-1}$ should result in a straight line whose y-intercept is v_∞. However, we did not find such linear behavior even for the longest times investigated, as shown in figure 3(a). Indeed, the additional logarithmic correction predicted in equation (4) can not be neglected. Assuming that

$$\partial_t \langle h \rangle \simeq v_\infty + s_\lambda \beta \Gamma^\beta \langle \chi \rangle t^{\beta-1} + s_\lambda \langle \zeta \rangle t^{-\delta} + \ldots, \tag{5}$$

the correction $s_\lambda \langle \zeta \rangle t^{-\delta}$ can be obtained by plotting $C \equiv \partial_t \langle h \rangle - v_\infty - s_\lambda \beta \Gamma^\beta \langle \chi \rangle t^{\beta-1}$ against time, as shown in the inset of figure 3(a). For all investigated models, we found the exponent $\delta = 1.01(1)$, consistent with the logarithmic correction, using $\langle \chi \rangle = \langle \chi_2 \rangle$ (GUE TW). Instead, if the GOE TW value is used, $\delta \approx 1 - \beta = 2/3$ is found (see the inset of figure 3(a)). This indicates that the term $t^{\beta-1}$ in equation (5) was not absorbed if the GOE TW value is assumed, giving further evidence that the GOE TW distribution does not correctly describe the distribution of χ.

The importance of the logarithmic term in equation (4) is evidenced when we try to determine the usual finite-time correction term η. Defining the variable

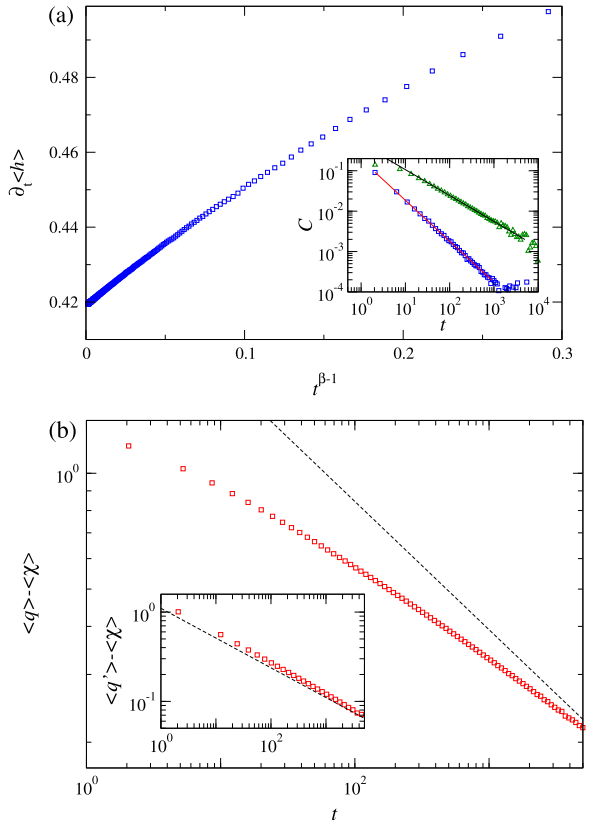

Figure 3. (a) Growth velocity versus $t^{\beta-1}$. The inset shows $C \equiv \partial_t\langle h\rangle - v_\infty - s_\lambda\beta\Gamma^\beta\langle\chi\rangle t^{\beta-1}$ against t with $\langle\chi\rangle = \left\langle \chi_1 \right\rangle$ (green triangles) and $\langle\chi\rangle = \left\langle \chi_2 \right\rangle$ (blue squares). The lines are results of power-law regressions. (b) Finite-time correction in the mean height versus time, disregarding (main plot) or considering (inset) the logarithmic correction (see text). The dashed lines indicate the slope $-1/3$. All the foregoing data were obtained for the RSOS model with $\omega = 20$.

$$q \equiv \frac{h - v_\infty t}{s_\lambda(\Gamma t)^\beta},$$

the finite-time correction in the mean height has a power-law decay, $\langle q\rangle - \langle\chi\rangle \sim t^{-\beta}$, for $\omega = 0$ [6, 7, 15, 18–20, 24]. However, for $\omega > 0$, a power-law decay is not found due to logarithmic correction, as shown in figure 3(b). Instead, including the logarithm term as

$$q' \equiv \frac{h - v_\infty t - s_\lambda\langle\zeta\rangle \ln t}{s_\lambda(\Gamma t)^\beta}, \tag{6}$$

and using the value of $\langle\zeta\rangle$ estimated from the power-law regressions shown in the inset of figure 3(a), the finite-time correction decaying as $t^{-\beta}$ is recovered (see inset of figure 3(b)). Moreover, we observe that $\langle\zeta\rangle$ does not significantly depend on ω and take values $\langle\zeta\rangle = 0.18(1)$, $0.15(4)$, and $0.22(3)$ for the RSOS, SS, and etching models, respectively, for ω varying from 1 to 100. Our analysis does not permit a conclusive assessment of logarithmic corrections in higher-order cumulants of height distribution. For the SS model, for which $\Gamma = 1/2$ is exactly known, $\langle h^n\rangle_c - [s_\lambda(\Gamma t)^\beta]^n\langle\chi^n\rangle_c$ seems to reach a constant value, suggesting

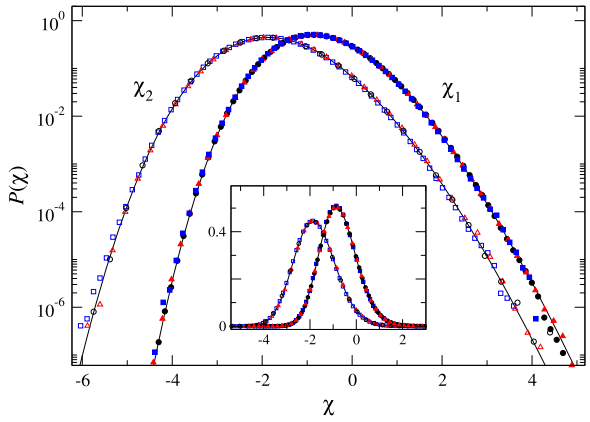

Figure 4. Rescaled height distributions for the RSOS (black circles), SS (red triangles), and etching (blue squares) models, with $\omega = 20$ (open symbols) for times $t = 18000$, 19000, and 15000, respectively, and with $\omega = 0$ (solid symbols) for $t = 2000$, 2000, and 1500, respectively. The main plot and the inset show these data in semi-log and linear scales, respectively. Here histograms of $\chi \equiv (h - v_\infty t - \langle\eta\rangle - s_\lambda \zeta \ln t)/(\Gamma t)^\beta$ are compared with the probability density of χ_1 and χ_2.

that ζ is deterministic. For RSOS, a very small variance $\langle\zeta^2\rangle_c \approx 0.005$, smaller than the uncertainties obtained with our current precision in Γ, is found.

Similarly to $\langle\zeta\rangle$, $\langle\eta\rangle$ also seems to be independent of ω: we found $\langle\eta\rangle = -0.87(3)$, -0.44 (3), and 3.2(2) for the RSOS, SS, and etching models, respectively, for the values of ω we investigated ($\omega \gtrsim 1$). However, they are larger (in the absolute value) than the estimates for $\omega = 0$, which are $\langle\eta\rangle = -0.32(4)$ for the RSOS model [15], and $\langle\eta\rangle = -0.33(1)$ for the SS model and $\langle\eta\rangle = 0.20(3)$ for the etching model (this work). Note that, for short times, the surface roughness is very small and duplication of columns does not have a significant effect on the mean height, so $\langle h\rangle_{\omega>0} \approx \langle h\rangle_{\omega=0}$ for short times. This suggests that $\langle\eta\rangle$ becomes larger for $\omega > 0$ so as to compensate for the change in the mean height due to the crossover from the GOE TW distribution to the GUE counterpart (see section 7).

Height distributions rescaled according to equation (4) are presented in figure 4. Excellent data collapse with the theoretical curve for the GUE TW distribution demonstrates that the asymptotic height fluctuations of flat models on growing substrates are given by the GUE TW distribution. The distributions for the same models with $\omega = 0$ are also shown for the sake of comparison. It is important to remark that rescaled height distributions without taking into account logarithmic correction display a shift in the mean, decaying very slowly as $\ln(t)/t^\beta$.

4. Height fluctuations in 2 + 1 dimensions

For two-dimensional enlarging substrates, we used $L_0 = \omega$ in both directions, with ω varying from 1 to 10, and averages were taken over 40 000 samples.

Figure 5(a) shows the evolution of the interface width ($W \equiv \sqrt{\langle h^2\rangle_c}$) over time and the corresponding effective growth exponent. Analogously to the one-dimensional case, the growth exponent values converge to that of the KPZ class in $d = 2 + 1$ dimensions, $\beta \approx 0.24$ [35]. The asymptotic growth velocities v_∞ for the three models with $\omega = 0$ were calculated in [24] (see table 1). For $\omega > 0$, we find a behavior of $\partial_t\langle h\rangle$ analogous to that for $d = 1 + 1$ (figure 3(a)),

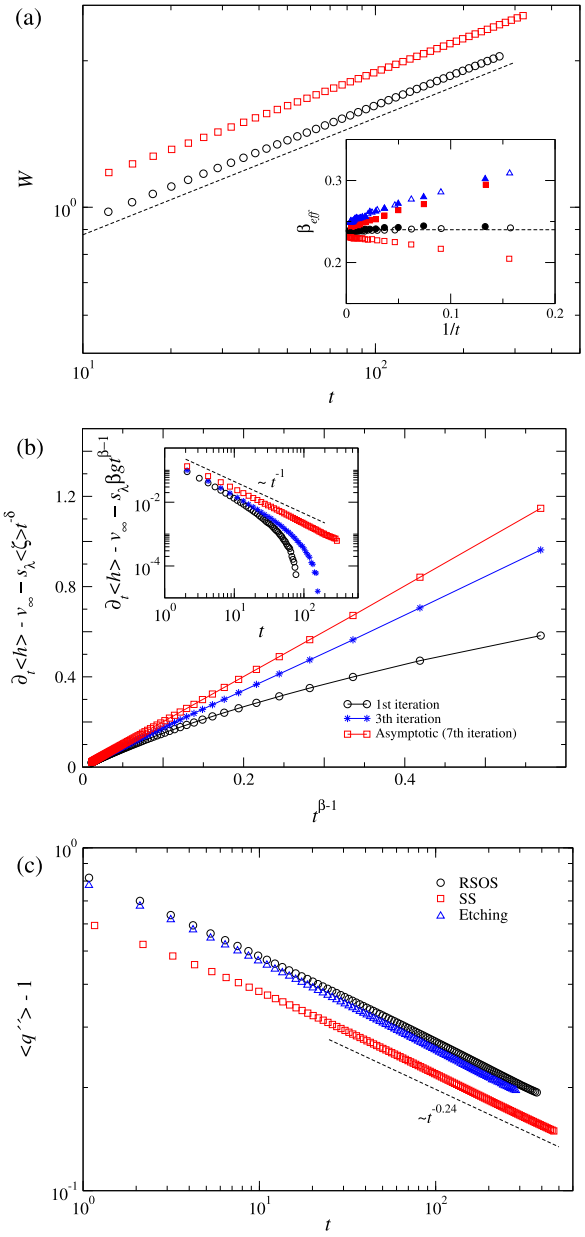

Figure 5. (a) Interface width versus time for the RSOS (black circles) and SS (red squares) models, with $\omega = 10$. The inset shows the effective growth exponents for the RSOS, SS, and etching (blue triangles) models, with $\omega = 6$ (solid symbols) and 10 (open symbols). The dashed line has the slope $\beta = 0.24$. (b) Illustration of the method to self-consistently determine $g \equiv \Gamma^{\beta}\langle\chi\rangle$ (main plot) and $\langle\zeta\rangle t^{-\delta}$ (inset) for the RSOS model with $\omega = 6$. We start the first iteration with $\langle\zeta\rangle t^{-\delta} = 0$. (c) Shift in rescaled mean height versus time for the three models with $\omega = 6$.

but since here the exact value of $\langle\chi\rangle$ is not known, we determine $\langle\zeta\rangle$ and δ in equation (5) in an iterative way as follows. Plotting $\partial_t\langle h\rangle - v_\infty$ against $t^{\beta-1}$, we estimate a rough value for the product $g \equiv \Gamma^{\beta}\langle\chi\rangle$ from the slope near the origin (figure 5(b)). We then use this *approximate* value to plot $\partial_t\langle h\rangle - v_\infty - s_\lambda\beta g t^{\beta-1}$ against t in logarithmic scales (inset of figure 5(b)), as done

Table 1. Non-universal (v_∞, λ, A and Γ) and universal ($\langle\chi\rangle_c$, $\langle\chi^2\rangle_c$, S, and K) quantities for different models on enlarging $d = 2 + 1$ dimensional substrates. The averages and uncertainties of universal quantities were determined using different substrate expansion rates $\omega > 0$.

	v_∞ [24]	λ	A	Γ	$\langle\chi\rangle_c$	$\langle\chi^2\rangle_c$	S	K
RSOS	0.31270(1)	-0.405(7)	1.22(4)	0.68(6)	-2.34(3)	0.341(5)	0.328(4)	0.210(4)
SS	0.341368(3)	-0.481(3)	1.44(5)	1.2(1)	-2.37(5)	0.336(6)	0.329(7)	0.206(3)
Etching	3.3340(1)	2.147(4)	3.629(9)	58.5(5)	-2.36(3)	0.346(8)	0.336(6)	0.21(1)

in figure 3(a). We expect this to decay as $\langle\zeta\rangle t^{-\delta}$ with $\delta > 1 - \beta$, but because of the error in the estimate of g, the residual on the order of $t^{\beta-1}$ dominates for large t. Therefore, $\langle\zeta\rangle$ and δ can be estimated from the data at small t. With these estimates, we reestimate g by plotting $\partial_t\langle h\rangle - v_\infty - s_\lambda\langle\zeta\rangle t^{-\delta}$ against $t^{\beta-1}$ (see again the main panel of figure 5(b)). Repeating this procedure to improve the estimates g, $\langle\zeta\rangle$, δ until they reach some asymptotic values, we finally find straight lines in both plots (red squares), which guarantee the self-consistency of the estimates. In particular, we find $\delta \approx 1$, which indicates the presence of a logarithmic correction in the KPZ ansatz for $d = 2 + 1$ also, as expected by the theoretical argument presented in section 2. As in $d = 1 + 1$, $\langle\zeta\rangle$ is almost independent of ω within the range of ω studied here, taking values at $\langle\zeta\rangle = 0.32(2), 0.36(4), 0.39(2)$ for the RSOS, SS, and etching models, respectively.

To determine $\langle\eta\rangle$, following [15, 24], we define the variable

$$q'' \equiv \frac{h - v_\infty t - s_\lambda\langle\zeta\rangle \ln t}{s_\lambda g t^\beta} \tag{7}$$

so that $\langle q''\rangle - 1 \simeq (s_\lambda\langle\eta\rangle/g)t^{-\beta}$. Figure 5(c) shows this shift against time, where the expected decay $t^{-\beta}$ is observed, and using the values of g obtained earlier, we estimate $\langle\eta\rangle$ at $\langle\eta\rangle = -1.8(2), -1.4(1)$, and $4.9(1)$ for the RSOS, SS, and etching models, respectively. These values are again independent of ω within $1 \leqslant \omega \leqslant 10$ and larger than the values for $\omega = 0$ (see table I in [24]).

The parameter Γ is given by $\Gamma = (1/2)|\lambda|A^{1/\alpha} = |\lambda|A^2/2$ for $d = 1 + 1$ dimensions and $\Gamma = |\lambda|A^{1/\alpha}$ for $d = 2 + 1$ dimensions, where A is defined by the steady-state growth velocity $v_s(L)$ in a system of (fixed) size L, through $v_s(L) - v_s(\infty) = -(\lambda A/2)L^{2\alpha-2}$ [26, 34, 36]. Note that the presence or absence of the factor 1/2 in the preceding expressions for Γ is not essential but is introduced only to conform with the definitions adopted in past studies. The parameter λ can be obtained from the dependence of the asymptotic growth velocity on the substrate slope u [36]; specifically, $\lambda = \left(\frac{\partial^2 v_\infty}{\partial u^2}\right)_{u\to 0}$. Therefore, by plotting $v_s(L) - v_s(\infty)$ against $L^{2\alpha-2}$ with the value $\alpha = 0.39$ for the (2+1)-dimensional KPZ class [35, 37], and by using all the foregoing expressions, we determined A and Γ as listed in table 1.

Using the estimated parameter values to rescale the height as in equation (6), universality in the height distribution for $d = 2 + 1$ can be explicitly assessed. The mean and the variance of χ are obtained from extrapolations of $\langle q'\rangle$ and $\langle q'^2\rangle_c$ against $t^{-\beta}$ and $t^{-2\beta}$, respectively, as shown in the insets of figure 6(a). Table 1 summarizes the values obtained by using different substrate expansion rates $\omega > 0$. These values are in good agreement with those obtained by Halpin–Healy [22, 23] for curved interfaces and far from those for flat ones. Therefore, the underlying

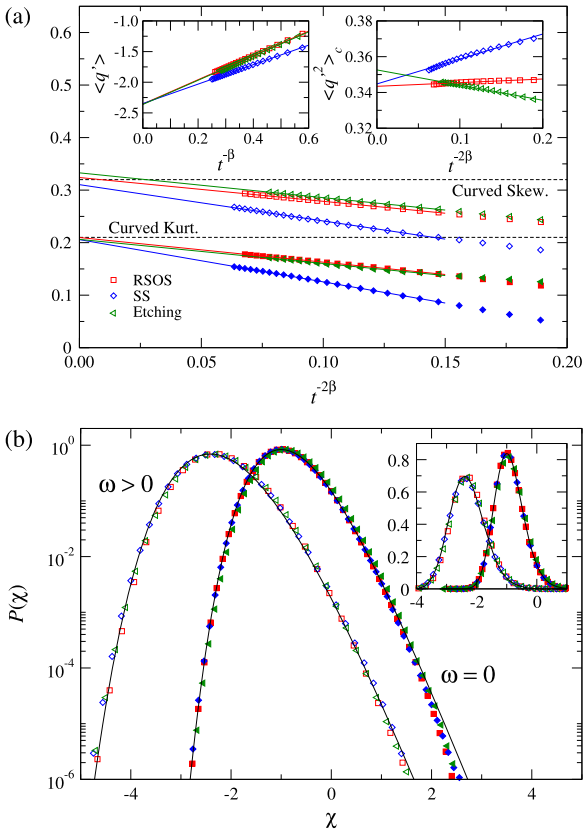

Figure 6. (a) Skewness (open) and kurtosis (solid symbols) against $t^{-2\beta}$for all investigated models with $\omega = 10$. Insets show $\langle q' \rangle$ (left) and $\langle q'^2 \rangle_c$ (right) versus $t^{-\beta}$ and $t^{-2\beta}$, respectively, for the same models. (b) Rescaled height distributions for the RSOS, SS, and etching models, with $\omega = 4$ (open symbols) and times $t = 500$, 650, and 350, respectively, and, with $\omega = 0$ (solid symbols) and $t = 10000$, 8000, and 2000, respectively. The main panel and the inset show these data in semi-log and linear scales, respectively. The solid lines are generalized Gumbel distributions with $m = 9.5$ (left) and $m = 6.0$ (right) [24].

fluctuations in two-dimensional enlarging substrates are also equivalent to those found for curved systems. This is corroborated by the skewness and the kurtosis of the height distributions, which converge to the corresponding values for the curved interfaces, as shown in figure 6(a) and table 1. It is worth stressing again that the global curvature of the interfaces is identically null, as in $d = 1 + 1$.

Finally, the height distributions rescaled according to equation (4) are shown in figure 6(b), where the excellent data collapse gives another evidence for their universality. Figure 6(b) also shows the generalized Gumbel distribution with parameter $m = 9.5$ (with $S = 0.332$ and $K = 0.221$ and rescaled to mean -2.33 and variance 0.34)[4], which is a good fit of χ for the curved KPZ subclass in $d = 2 + 1$ [24]. Moreover, rescaled distributions for $\omega = 0$ are shown

[4] Although the generalized Gumbel distributions with $m = 6.0$ and 9.5 serve as good fits to the distribution for the flat and curved KPZ subclasses, respectively, in $d = 2 + 1$ dimensions [24], no theoretical argument suggests that they are the true asymptotic distributions. Therefore, the values of their skewness and kurtosis are not exactly those for the KPZ class. For the KPZ class values, one should refer to numerical estimates, reported in [22–24].

in figure 6(b), which clearly show the existence of two different universal distributions for the underlying fluctuations of fixed-size and enlarging substrate KPZ subclasses in $d = 2 + 1$. Again, the generalized Gumbel distribution, with parameter $m = 6.0$ (with $S = 0.424$ and $K = 0.359$ and rescaled to mean -0.90 and variance 0.24 (see footnote 4), provides a good fit of χ for almost five decades around the peak, as also observed in [24].

5. Spatial covariance

Beyond the asymptotic height distribution, the limiting processes that describe the spatial profile of the flat and curved KPZ-class interfaces are exactly known in 1 + 1 dimensions and are called the Airy_1 and Airy_2 processes, respectively [14, 38]. We calculate the spatial covariance

$$C_s(r, t) = \left\langle \tilde{h}(x, t)\tilde{h}(x + r, t) \right\rangle \simeq (\Gamma t)^{2\beta} \Psi\left[A_h r / (\Gamma t)^{2\beta}\right], \tag{8}$$

where $\tilde{h} \equiv h - \langle h \rangle$, Ψ is a scaling function, and $A_h = A$ in 1 + 1 and $A_h = 0.6460A$ in 2 + 1 dimensions [26]. Figure 7(a) shows the rescaled spatial covariance for $d = 1 + 1$ along with the Airy_1 and Airy_2 covariances. We find that the results for $\omega > 0$ and $\omega = 0$ are in good agreement with the Airy_2 and Airy_1 covariances, respectively, showing that the equivalence between expanding substrate systems and curved interfaces also holds for the spatial correlation.

In $d = 2 + 1$, the spatial covariance for flat interfaces was numerically calculated only very recently [26] and was shown to be universal, as is the case for $d = 1 + 1$. However, there were no reports on the spatial covariance for curved interfaces until this work. Here we determined the spatial covariance for the investigated models for both $\omega = 0$ and $\omega > 0$. The rescaled curves are presented in figure 7(b), where two universal curves for fixed-size and enlarging substrates are observed. These can be regarded as the (2+1)-dimensional analog of the Airy_1 and Airy_2 covariances, respectively. For the etching model on enlarging substrates, the rescaled curves do not converge yet within the examined time window, but are still approaching the asymptotic curve obtained for the RSOS and SS models (see the inset of figure 7).

6. Temporal covariance

Similarly to the spatial case, we can define the temporal covariance

$$C_t(t, t_0) = \left\langle \tilde{h}(x, t_0)\tilde{h}(x, t) \right\rangle, \tag{9}$$

which is expected to scale as $C_t(t, t_0) \simeq (\Gamma^2 t_0 t)^{\beta} \Phi(t/t_0)$ [7, 39, 40]. As with the results for the spatial correlation, it is reasonable to expect that the scaling function $\Phi(x)$ is universal within each subclass and dimensionality. However, unlike the spatial correlation, no exact results have been obtained for the temporal correlation, even for $d = 1 + 1$. Therefore, it is very important to check their universality by empirical approaches, such as simulations and experiments.

Figure 8(a) shows the rescaled temporal covariance for all investigated models in $d = 1 + 1$ on fixed-size and enlarging substrates, along with the experimental data for flat and curved interfaces generated in the electroconvection of nematic liquid crystals [6, 7] (already reported in [7]). For fixed-size substrates, good collapse of data for all models and initial times t_0 is observed. Moreover, good agreement between the numerical and experimental covariances

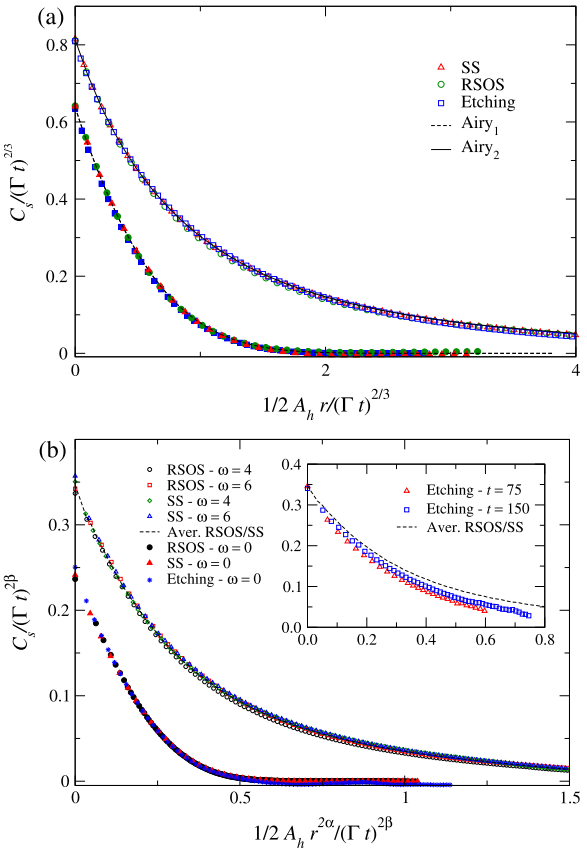

Figure 7. (a) Rescaled spatial covariances for all investigated models in $d = 1 + 1$ with $\omega = 0$ (solid) and $\omega = 20$ (open symbols), for times $t = 4000$ and 10000, respectively. (b) Rescaled spatial covariances in $d = 2 + 1$ dimensions, for times $t = 600$ ($\omega = 0$), $t = 250$ ($\omega = 4$), and $t = 150$ ($\omega = 6$). Results for the etching model on enlarging substrates are shown in the inset at two different times. The exponents $\alpha = 0.395$ and $\beta = 0.237$ were used for the rescaling.

is found. For enlarging substrates, the temporal covariances for the RSOS and SS models already reach an asymptotic function, clearly different from that for the fixed-size case, whereas the finite-time effect seems to be more severe for the etching model, similar to the spatial covariance as reported in the inset of figure 7(b). A similar effect was also observed for the curved interfaces in the liquid-crystal experiment (see the inset of figure 11(b) in reference [7]).

To substantiate that the deviation from the asymptotic form is indeed a finite-time effect, we attempt an extrapolation of the finite-time data as follows. Assuming that η is stochastic (as shown by past studies [7, 15, 20, 33]) and neglecting ζ fluctuations (as discussed earlier), we expect from the KPZ ansatz (equation 4) that the leading correction in Φ is on the order of $t^{-\beta}$. Using this expression and data at two different t_0 with fixed t/t_0, we can extrapolate to obtain the asymptotic temporal covariance Φ. The data for the etching model in the main panel of figure 8(a) are obtained in this way from the raw data in the inset, and excellent agreement with the raw data for the RSOS and SS models is achieved. For the experimental data of the curved interfaces, the same quality of collapse and agreement is obtained by assuming that the leading finite-time correction to Φ is $\mathcal{O}(t_0^{-2\beta})$. This may be related to the vanishing finite-time

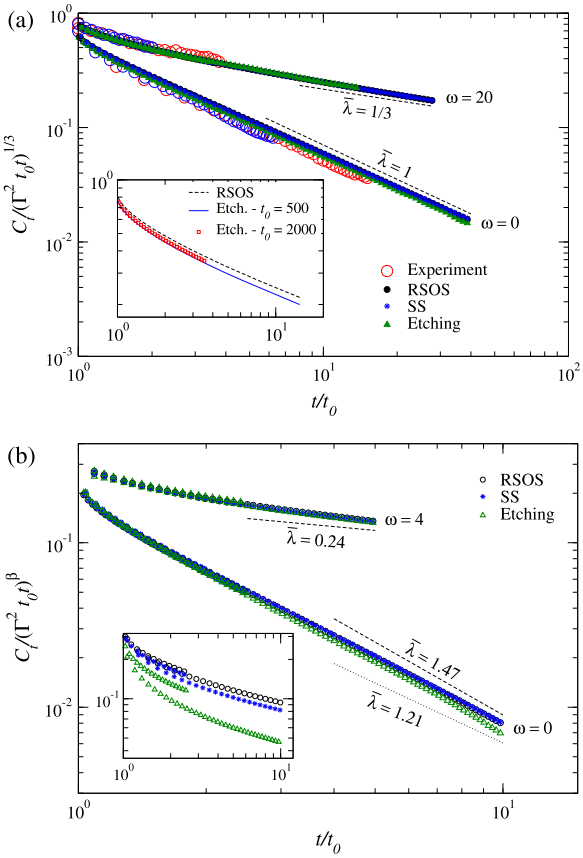

Figure 8. (a) Rescaled temporal covariance for all investigated models (solid symbols) in $d = 1 + 1$ and the liquid-crystal experiment (open symbols) with flat and curved interfaces. In both cases, different initial times t_0 in the range [100, 2000] (models) and [4*s*, 25*s*] (experiment) were used. For etching model and curved experimental surfaces, the curves are extrapolations. The raw data for etching model are shown in the inset. (b) Rescaled temporal covariances for all models in $d = 2 + 1$ dimensions and for different initial times. For $\omega = 4$, all curves in the main panel are extrapolations, whereas the non-extrapolated ones are shown in the inset.

correction for the one-point second-order cumulant $\langle \chi^2 \rangle_c$ for the curved case [7], but such a relationship needs to be clarified by further analytical and empirical studies.

In $d = 2 + 1$, for fixed-size substrates, we again find good collapse of rescaled (non-extrapolated) temporal covariances for all models and initial times, as shown in figure 8(b). However, for enlarging systems the finite-time effects are larger, and even for the RSOS and SS models we do not attain data collapse, as shown in the inset of figure 8(b). In these models, extrapolations for the correction $\mathcal{O}(t_0^{-\beta})$ fail to collapse the data, whereas a correction $\mathcal{O}(t_0^{-2\beta})$ provides a nice collapse for both models and for different times used for the extrapolation (figure 8(b)). For the etching model, good collapse of data is not achieved with the correction $\mathcal{O}(t_0^{-\beta})$ or $\mathcal{O}(t_0^{-2\beta})$. Instead, apparent collapse is achieved with an intermediate exponent $\mathcal{O}(t_0^{-0.32})$, possibly arising from a mixture of both the preceding terms, within the time window we investigated.

The strengths of the two correction terms, $\mathcal{O}(t_0^{-\beta})$ and $\mathcal{O}(t_0^{-2\beta})$, may be related to the finite-time correction to the second-order cumulant $\langle \chi^2 \rangle_c$. Indeed, the etching model, whose correction to the second-order cumulant is known to be large [41], also exhibits the large finite-time corrections to the temporal covariance as presented earlier. Although these two corrections are formally different because they concern equal-time and two-time properties, respectively, better understanding of such a relationship will certainly contribute to a more unambiguous determination of the universal functional forms for the temporal covariance.

In any case, our results in figure 8 show that the temporal covariance is clearly different between the fixed-size and enlarging systems, and that they agree, in $d = 1 + 1$ dimensions, with the results for the flat and curved interfaces, respectively, in the liquid-crystal experiment. The rescaled covariance $\Phi(t/t_0)$ converges to a universal function in each case and each dimensionality, as substantiated by the three models investigated here. Importantly, Kallabis and Krug [39] had conjectured that for long times $\Phi(x) \sim x^{-\bar{\lambda}}$ with $\bar{\lambda} = \beta + d_s/z$ for flat interfaces, whereas $\bar{\lambda} = \beta$ was later proposed for the curved interfaces [40]. Besides confirming these scaling relations in $d = 1 + 1$, our results suggest that they also seem to be valid for $d = 2 + 1$ (dashed lines in figure 8(b)), though clear power laws are not yet reached within the time studied. Note that our result for $\omega = 0$ seems to be consistent with the recent estimate $\bar{\lambda} = 1.21$ in [42] for intermediate times (dotted line in figure 8(b)), but it eventually becomes closer to the value indicated by Kallabis and Krug's conjecture, $\bar{\lambda} = 1.47$ (dashed line).

7. Crossover from fixed-size to enlarging substrates

Our enlarging-substrate systems are also convenient for studying crossover between the fixed-size/flat and enlarging/curved subclasses or, for $1 + 1$ dimensions, between the GOE and GUE TW distributions. Such inter-subclass crossover has also attracted great interest [14], both theoretically and experimentally. Analytical studies have mostly dealt with crossover in space for $1 + 1$ dimensions [14]: for example, Borodin *et al* [43] and Le Doussal [44] considered an initial condition composed of a flat substrate for $x < 0$ and a wedge (curved) one for $x > 0$, and formulated crossover from the GOE to the GUE TW distribution, or from the Airy_1 to the Airy_2 process, which takes place as one moves from $x \to -\infty$ to $x \to \infty$. In contrast, crossover in time remains out of the reach of analytical studies, as it requires understanding of the temporal covariance, but it has been recently addressed numerically and experimentally for the crossover from flat to stationary subclasses [23, 45, 46]. Here we investigate temporal crossover from fixed-size/flat to enlarging/curved subclasses (from GOE to GUE TW for $d = 1 + 1$) by starting with an initial substrate such that $L_0 \gg \omega$. As the mean substrate size grows as $\langle L \rangle = L_0 + \omega t$, the characteristic crossover time is given by $t^* \sim L_0/\omega$. We therefore expect that, for $t \ll t^*$ (or equivalently $\omega \to 0$ or $L_0 \to \infty$), the system essentially behaves as a fixed-size system, whereas for $t \gg t^*$ the statistical properties of the enlarging/curved systems should take over.

This scenario is indeed consistent with our results shown in figures 9(a) and (b), where the skewness S and kurtosis K of the one-dimensional RSOS model are plotted as functions of $\langle L \rangle / L_0 \simeq t/t^*$. The cumulant ratios reach maxima near $t = t^*$, at some values close to those for the GOE TW distribution, and then approach the GUE TW values. As expected, the larger L_0 becomes, the closer the maximal values of the cumulant ratios are to the GOE TW values. Interestingly, these maxima $S_{\max}(L_0)$ and $K_{\max}(L_0)$ are found to vary linearly with $L_0^{-\beta}$

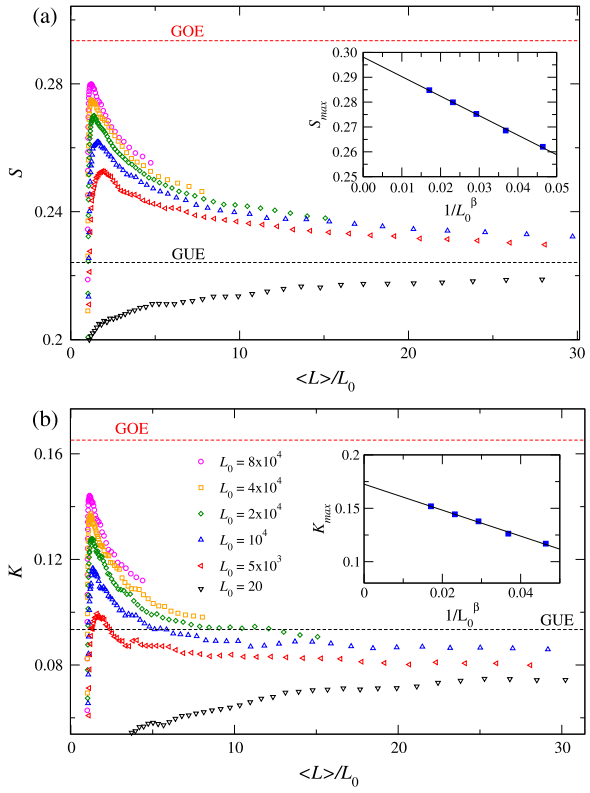

Figure 9. Evolution of (a) the absolute value of the skewness and (b) the kurtosis for the one-dimensional RSOS model with $\omega = 20$ and different initial system sizes. The insets show the maximal values against $L_0^{-\beta}$, with linear extrapolations to the asymptotic values.

(insets). This allows us to extrapolate the asymptotic values $S_{\max}(\infty) = 0.297(4)$ and $K_{\max}(\infty) = 0.17(1)$, which agree with the GOE TW distribution ($S = 0.2935$, $K = 0.1652$). Similar results were also obtained for all models in $2 + 1$ dimensions (data not shown).

8. Conclusions

In this article, we studied typical models of the KPZ class on flat substrates enlarging at a constant rate ω. Although the growth exponent β is the same for fixed-size ($\omega = 0$) and enlarging ($\omega > 0$) substrates, the height distribution does change: for the fixed-size case, it is given by the universal distribution for flat interfaces (GOE TW in $d = 1 + 1$), whereas for the enlarging case the distribution for curved interfaces arises (GUE TW in $d = 1 + 1$). We also reached the same conclusion for the spatial and temporal covariances. In particular, we found the Airy_1 and Airy_2 covariances for the spatial correlation of the fixed-size and enlarging systems in $d = 1 + 1$, respectively, as well as agreement with the Kallabis-Krug conjecture on the temporal covariance [7, 39, 40]. Moreover, we also studied $(2 + 1)$-dimensional systems and found clear agreement in the height distribution, with the functional forms previously obtained numerically for curved and flat interfaces.

All these results indicate that the interfaces growing on enlarging substrates share the same statistical properties as the curved interfaces, despite the fact that the global curvature in these

enlarging systems is kept exactly null. This suggests that substrate enlargement is possibly more relevant for the realization of the 'curved interface' subclass than the global curvature itself. Indeed, to our knowledge, all interfaces deemed 'curved' in previous work (e.g., [6, 7, 13, 14, 21, 24, 47, 48]) evolve within a zone of activity that grows linearly over time. The activity zone corresponds to the growing circumference for the usual circular interfaces, but this concept is also valid for the asymmetric simple exclusion process with the step initial condition [47, 48], in which particles can move only within a linearly growing area around the origin. We hope that the relevance of such substrate enlargement to the 'curved interface' subclass will be further investigated on a mathematical or theoretical basis; for this, the so-called characteristic lines [49, 50], which describe the directions of the fluctuation propagation in space-time, may be a useful concept.

Beyond those asymptotic universal quantities, finite-time behavior was also characterized. We found a logarithmic correction in the height evolution (equation 4) when the substrate is enlarging. We consider that this correction is a consequence of column duplications adopted in our time evolution rule for enlarging substrates. Furthermore, crossover from the fixed-size (flat) to the enlarging substrate (curved) subclasses (GOE to GUE TW distributions in $d = 1 + 1$), which takes place in the course of time evolution, has also been characterized.

As a final remark, we stress that our simulation method based on substrate enlargement provides a powerful tool to study statistical properties of the curved interface subclass since this produces isotropic interfaces on a lattice. This is not the case of the usual growth models on lattice, such as the Eden model, which is known to produce an anisotropic interface even from a single point seed [15, 51, 52], reflecting the lattice structure of the model. Having access to isotropic interfaces instead is essential for studying statistical properties of interest numerically because then we can use all spatial points to improve statistics and to define the spatial correlation functions unambiguously. Indeed, in this article, this allowed us to determine the two-point spatial correlation function for enlarging/curved systems in $2 + 1$ dimensions for the first time. Our method of enlarging substrates therefore provides a useful platform to study statistical properties of the KPZ class in higher dimensions, and of other universality classes for fluctuating surface growth problems.

Acknowledgments

The authors thank R Cuerno and I Corwin for helpful discussions. This work is supported in part by CNPq, CAPES, and FAPEMIG (Brazilian agencies) and by KAKENHI (no. 25707033 from JSPS and no. 25103004, 'Fluctuation & Structure' from MEXT, Japan).

References

[1] Barabasi A-L and Stanley H E 1995 *Fractal Concepts in Surface Growth* (Cambridge: Cambridge University Press)
[2] Meakin P 1998 *Fractals, Scaling and Growth far from Equilibrium* (Cambridge: Cambridge University Press)
[3] Evans J W, Thiel P A and Bartelt M C 2006 *Surf. Sci. Rep.* **61** 1–128
[4] Pimpinelli A and Villain J 1998 *Physics of Crystal Growth* (Cambridge: Cambridge University Press)
[5] Vicsek T, Cserzö M and Horváth V K 1990 *Physica* A **167** 315–21
Brú A, Pastor J M, Fernaud I, Brú I, Melle S and Berenguer C 1998 *Phys. Rev. Lett.* **81** 4008–11

Galeano J, Buceta J, Juarez K, Puramiño B, de la Torre J and Iriondo J M 2003 *Europhys. Lett.* **63** 83
Huergo M A C, Pasquale M A, González P H, Bolzán A E and Arvia A J 2012 *Phys. Rev.* E **85** 011918
[6] Takeuchi K A and Sano M 2010 *Phys. Rev. Lett.* **104** 230601
Takeuchi K A, Sano M, Sasamoto T and Spohn H 2011 *Sci. Rep.* **1** 34
[7] Takeuchi K and Sano M 2012 *J. Stat. Phys* **147** 853–90
[8] Yunker P J, Lohr M A, Still T, Borodin A, Durian D J and Yodh A G 2013 *Phys. Rev. Lett.* **110** 035501
[9] Krug J 2009 *Phys. Rev. Lett.* **102** 139601
[10] Masoudi A A, Hosseinabadi S, Davoudi J, Khorrami M and Kohandel M 2012 *J. Stat. Mech.* L02001
[11] Masoudi A A, Khorrami M, Stastna M and Kohandel M 2012 *Europhys. Lett.* **100** 16004
[12] Ferreira S C and Alves S G 2006 *J. Stat. Mech.* P11007
[13] Prähofer M and Spohn H 2000 *Phys. Rev. Lett.* **84** 4882–5
[14] For recent reviews on theoretical developments on the KPZ class, see, e.g., Kriecherbauer T and Krug J 2010 *J. Phys.* A **43** 403001
Corwin I 2012 *Random Matrices Theor. Appl.* **1** 1130001
[15] Alves S G, Oliveira T J and Ferreira S C 2013 *J. Stat. Mech.* P05007
[16] Tracy C and Widom H 1994 *Commun. Math. Phys.* **159** 151–74
[17] Kardar M, Parisi G and Zhang Yi C 1986 *Phys. Rev. Lett.* **56** 889–92
[18] Alves S G, Oliveira T J and Ferreira S C 2011 *Europhys. Lett.* **96** 48003
[19] Takeuchi K A 2012 *J. Stat. Mech.* P05007
[20] Oliveira T J, Ferreira S C and Alves S G 2012 *Phys. Rev.* E **85** 010601
[21] Sasamoto T and Spohn H 2010 *Phys. Rev. Lett.* **104** 230602
Amir G, Corwin I and Quastel J 2011 *Commun. Pure Appl. Math.* **64** 466
Calabrese P and Le Doussal P 2011 *Phys. Rev. Lett.* **106** 250603
Imamura T and Sasamoto T 2012 *Phys. Rev. Lett.* **108** 190603
[22] Halpin-Healy T 2012 *Phys. Rev. Lett.* **109** 170602
[23] Halpin-Healy T 2013 *Phys. Rev.* E **88** 042118
[24] Oliveira T J, Alves S G and Ferreira S C 2013 *Phys. Rev.* E **87** 040102
[25] Almeida R A L, Ferreira S O, Oliveira T J and Aarão Reis F D A 2014 *Phys. Rev.* B **89** 045309
[26] Halpin-Healy T and Palasantzas G 2014 *Europhys. Lett.* **105** 50001
[27] Alves S G, Oliveira T J and Ferreira S C 2014 *Phys. Rev.* E **90** 020103
[28] Pastor J M and Galeano J 2007 *Cent. Eur. J. Phys.* **5** 539
[29] Escudero C 2009 *J. Stat. Mech.* P07020
[30] Kim J M and Kosterlitz J M 1989 *Phys. Rev. Lett.* **62** 2289–92
[31] Mello B A, Chaves A S and Oliveira F A 2001 *Phys. Rev.* E **63** 041113
[32] van Beijeren H 1977 *Phys. Rev. Lett.* **38** 993
[33] Ferrari P L and Frings R 2011 *J. Stat. Phys.* **144** 1123–50
[34] Krug J, Meakin P and Halpin-Healy T 1992 *Phys. Rev.* A **45** 638–53
[35] Kelling J and Ódor G 2011 *Phys. Rev.* E **84** 061150
[36] Krug J and Meakin P 1990 *J. Phys. A: Math. Gen.* **23** L987
[37] Marinari E, Pagnani A and Parisi G 2000 *J. Phys. A: Math. Theor.* **33** 8181
[38] Prähofer M and Spohn H 2002 *J. Stat. Phys.* **108** 1071–106
Sasamoto T 2005 *J. Phys. A: Math. Theor.* **38** L549
Borodin A, Ferrari P and Sasamoto T 2008 *Commun. Math. Phys.* **283** 417–49
[39] Kallabis H and Krug J 1999 *Europhys. Lett.* **45** 20
[40] Singha S B 2005 *J. Stat. Mech.* P08006
[41] Aarão Reis F D A 2004 *Phys. Rev.* E **69** 021610
[42] Ódor G, Kelling J and Gemming S 2014 *Phys. Rev.* E **89** 032146
[43] Borodin A, Ferrari P L and Sasamoto T 2008 *Commun. Pure Appl. Math.* **61** 1603–29
[44] Le Doussal P 2014 *J. Stat. Mech.* P04018

[45] Takeuchi K A 2013 *Phys. Rev. Lett.* **110** 210604
[46] Halpin-Healy T and Lin Y 2014 *Phys. Rev.* E **89** 010103
[47] Johansson K 2000 *Commun. Math. Phys.* **209** 437–76
[48] Tracy C A and Widom H 2009 *Commun. Math. Phys.* **290** 129–54
[49] Ferrari P L 2008 *J. Stat. Mech.* P07022
[50] Corwin I, Ferrari P L and Péché S 2012 *Ann. Inst. Henri Poincaré B Probab. Statist.* **48** 134–50
[51] Zabolitzky J G and Stauffer D 1986 *Phys. Rev.* A **34** 1523
[52] Paiva L R and Ferreira S C 2007 *J. Phys. A: Math. Theor.* **40** F43
[53] Ferrari P L, Prähofer M and Spohn H 2004 *Phys. Rev.* E **69** 035102
[54] Degawa M, Stasevich T J, Cullen W G, Pimpinelli A, Einstein T L and Williams E D 2006 *Phys. Rev. Lett.* **97** 080601
[55] For a recent review on the facet experiments, see Einstein T L and Pimpinelli A 2014 *J. Stat. Phys.* **155** 1178